arXiv:1409.1269v1 [cond-mat.mtrl-sci] 3 Sep 2014

Optical emulation of double-continuum Fano interference by circularly dichroic plasmonic metasurfaces

Nihal Arju, Tzuhsuan Ma, Alexander Khanikaev, David Purtseladze, and Gennady Shvets
Department of Physics and Institute for Fusion Studies,
The University of Texas at Austin, One University Station C1500, Austin, Texas 78712
(Dated: September 5, 2014)

Classical emulation of a ubiquitous quantum mechanical phenomenon of double-continuum Fano (DCF) interference using metasurfaces is experimentally realized by engineering the near-field interaction between two bright and one dark plasmonic modes. The competition between the bright modes, with one of them effectively suppressing the Fano interference for the orthogonal light polarization, is discovered and explained by the analytic theory of the plasmonic DCF interference, which is further applied to predicting the circularly dichroic optical field concentration by plasmonic metasurfaces.

PACS numbers: 78.67.Pt, 73.20.Mf, 81.05.Xj, 42.25.BS

Ugo Fano's breakthrough paper [1] that explained asymmetric ionization spectra in atomic systems by introducing the now eponymous interference between discrete and continuous states continues to be highly influential despite its publication more than half a century ago. Universal concepts of Fano resonance, interference, and lineshape have been applied to several areas of optical science, including photonics, plasmonic nanostructures, and metamaterials [2–6]. The sharp spectral features in Fano-resonant metamaterials, combined with strong optical field concentration, make them attractive for sensing/fingerprinting [7–10] and nonlinear [11, 12] applications.

Most of the recently reviewed [4, 5, 13] work on optical Fano resonances deals with near-field coupling between a single bright and a single dark resonances, respectively emulating the continuum and discrete atomic states. However, the original Fano paper addressed a much broader class of couplings between atomic states, including one discrete and multiple continuum states. The key difference between the single-continuum and double-continuum cases is that the ionization probability vanishes for at least some values of energy loss of the ionizing particle in the former but not in the latter case [1]. Thus, the magnitude of Fano interference can be suppressed by the second continuum state.

In this Letter, we report the realization of the optical analog of double-continuum Fano (DCF) interference using a circularly dichroic (CD) plasmonic metasurface shown in Fig. 1 which supports one dark and two bright plasmonic modes. The modes are controllably coupled to each in the near field through symmetry-breaking vertical displacement s_y of a horizontal nanorod coupler (HNC) from its symmetric position. Our experimental measurements of Fano-shaped polarized reflectivity spectra $R_{xx}(\lambda)$ and $R_{yy}(\lambda)$ shown in Fig. 2(a,b) reveal a new optical phenomenon of *continuum state competition* in asymmetric photonic structures: the presence of the second (e.g., $y-$polarized) continuum state can significantly affect the strength of the Fano interference of the dark state with the first (e.g., $x-$polarized) continuum state. Unlike the plasmonic phenomenon [14] of the Fano feature reduction by *non-radiative* (Ohmic) losses, the continuum state competition directly emulates the atomic systems [1] where the non-radiative decay rate of the discrete state is naturally negligible. This phenomenon was not addressed in the earlier optical DCF work [15, 16] because the relative mode coupling cannot be controlled in a fixed geometry structure.

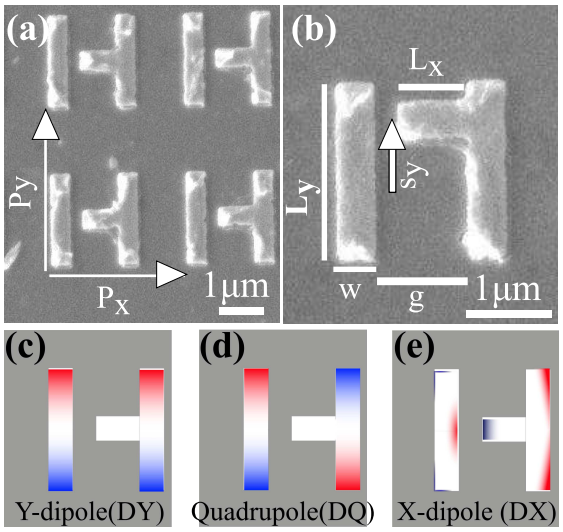

FIG. 1: (color online) (a) Scanning electron micrograph of a fabricated DCF metasurface. (b) Geometry definitions of a unit cell ($s_y = 0.52\mu$m). For all metasurfaces: $P_x = 2.7\mu m$, $P_y = 3.15\mu m$, $w = 0.36\mu m$, $L_x = 0.92\mu m$, $L_y = 1.8\mu m$, and $g = 0.66\mu m$. (d-f): Charge distributions of the three unperturbed eigenmodes of the symmetric ($s_y = 0$) metasurface. (d) and (f): bright DY and DX, (e): dark DQ.

Experimental results– A family of gold metasurfaces shown in Fig. 1 with different symmetry-breaking parameters s_y were fabricated on CaF_2 substrates using elec-

tron beam lithography. The lowest plasmonic resonances of the metasurfaces shown in Fig. 1 are classified as one dark quadrupolar (DQ) and two bright dipolar (DX and DY) plasmonic modes that are radiatively coupled to incident light polarized in the $x-$ and $y-$directions, respectively, giving rise to two quasi-continua of electromagnetic states. The finite displacement s_y of the HNC that perturbs the DQ mode is used to control the coupling between the modes. Polarized reflection coefficients were measured using Fourier transform infrared microspectroscopy. The $R_{yy}(\lambda)$ and $R_{xx}(\lambda)$ spectra shown in Fig. 2(a) reveal broad reflectivity peaks inside the shaded ($4.5\mu m < \lambda < 6\mu m$) spectral window, corresponding to the bright DY and DX resonances, respectively. In the rest of the Letter we concentrate on the $6\mu m < \lambda_{DQ}(s_y) < 8\mu m$ spectral window containing the dark DQ mode.

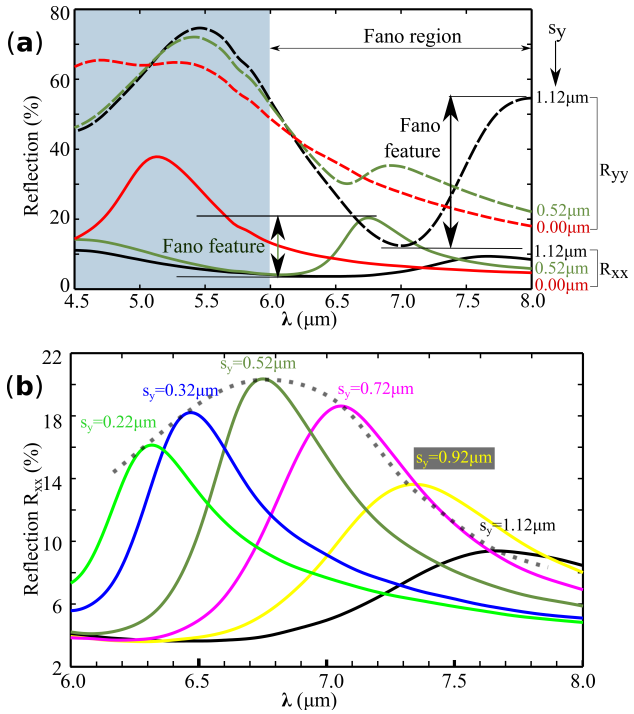

FIG. 2: (color online) (a) Measured reflectivity spectra R_{xx} (solid lines) and R_{yy} (dashed lines). Fano feature in R_{yy} is larger than in R_{xx} for $s_y = 1.12\mu$m (black line); opposite is true for $s_y = 0.52\mu$m (green line). Fano features are absent for $s_y = 0$ (red lines). (b) Zoomed-in R_{xx} spectra for 0.22μm$< s_y < 1.22\mu$m. Dotted line: non-monotonic behavior of the Fano feature with s_y interpreted as the competition between $x-$ and $y-$polarized continua.

Several key observations can be made based on the spectral Fano features measured for a wide range of the symmetry-breaking parameter s_y. *First,* we conclude from Fig. 2(a) that the relative coupling strengths $\tilde{\kappa}_{XQ}(s_y)$ (between DQ and DX) and $\tilde{\kappa}_{YQ}(s_y)$ (between DQ and DY) vary widely with s_y. This conjecture follows from the very different manifestations of Fano resonance in R_{xx} and R_{yy} spectra. Specifically, for small values of $s_y < L_y/4$, the Fano feature in the $x-$polarization becomes strongly pronounced while it is barely noticeable in $y-$polarization (e.g., $s_y = 0.52\mu$m). The opposite is true for large values of s_y: the Fano feature in $R_{yy}(\lambda)$ is much stronger than in $R_{xx}(\lambda)$ for $s_y \geq L_y/2$ (e.g., $s_y = 1.12\mu$m).

Second, we observe from Fig. 2(b) that the magnitude of the Fano feature in x-polarization is non-monotonic in s_y. The peak value of R_{xx} (dotted line) plotted in Fig. 2(b) increases with s_y, reaches the maximum at $s_y \equiv s_y^{\max} \approx 0.52\mu$m, and decreases for $s_y > s_y^{\max}$. The decrease of the Fano feature for large values of s_y is unexpected because the coupling coefficient $\tilde{\kappa}_{XQ}(s_y)$ continues monotonically increasing with s_y even for $s_y > s_y^{\max}$. The observed decrease is the direct experimental evidence of continuum state competition in DCF originally predicted by Fano [1] for atomic systems. Specifically, the linewidth $\delta\lambda_{DQ}(s_y)$ of the radiatively-broadened Fano resonance increases (and the corresponding quality factor $Q(s_y) = \lambda_{DQ}/(\delta\lambda_{DQ})$ decreases) faster with s_y than the coupling coefficient $\tilde{\kappa}_{XQ}(s_y)$, thereby suppressing the Fano feature in R_{xx}.

Theoretical model of DCF in plasmonic metasurfaces– To explain these experimental results and to explore the possibility of circularly dichroic optical field concentration, in what follows we develop a simple analytic model of optical DCF. The interaction of light with the three modes (two quasi-continuum and one discrete) of the metasurface is described by the following equations based on the [17, 18] coupled mode theory (CMT):

$$\begin{aligned} \frac{dD_Y}{dt} &= i\tilde{\omega}_Y D_Y + i\kappa_{XY} D_X + \alpha_y E_y^{in} \\ \frac{dQ}{dt} &= i\tilde{\omega}_Q Q + i\kappa_{XQ} D_X \\ \frac{dD_X}{dt} &= i\tilde{\omega}_X D_X + i\kappa_{XY} D_Y + i\kappa_{XQ} Q + \alpha_x E_x^{in}, \quad (1) \end{aligned}$$

where D_X, D_Y, and Q are the mode amplitudes, and $\alpha_{x(y)}$ are the radiative coupling efficiencies of the bright resonances to the far-field $x(y)-$polarized incident waves with amplitudes $E_{x(y)}^{in}$, respectively. The three modes are characterized by their complex-valued unperturbed eigenfrequencies $\tilde{\omega}_{X,Q,Y} \equiv \omega_m - i\tau_m^{-1}$ ($m = X, Y, Q$ is the resonance's index), where ω_m and τ_m are the spectral position and unperturbed lifetime of the m'th mode, respectively.

Note that the κ_{YQ} component of the near-field coupling tensor κ_{lm} has been neglected in Eq.(1) in comparison with its $\kappa_{XQ}(s_y)$ and $\kappa_{XY}(s_y)$ components for small value of s_y. Qualitatively, κ_{lm} is proportional to the overlap integral $\vec{E}_l \cdot \vec{E}_m$ inside the region occupied by the HNC. In can be observed from Fig. 1(d-f) that (a) E_x is the largest electric field component for all three modes in the said region of space, and (b) $E_x = 0$ at $y = 0$ for the DQ and DY modes. Therefore, it is ex-

pected that $\kappa_{XQ}, \kappa_{XQ} \propto s_y$, but $\kappa_{YQ} \propto s_y^2$ can be neglected for $s_y \ll L_y/4$. Also, from the energy conservation [13, 17, 42], $1/\tau_{X,Y} = |\alpha_{x,y}|^2 + 1/\tau_{X,Y}^{\rm Ohm}$, where $1/\tau_{X,Y}^{\rm Ohm}$ are the intrinsic decay rates.

After solving Eq.(1) in the vicinity of the dark resonance under the small-coupling ($|\kappa_{XY}|, |\kappa_{XQ}| \ll |\omega_Q - \omega_{X,Y}|$) assumption and using the expressions for the complex-valued reflection amplitudes [13] $r_{xx(yy)} = \alpha_{x(y)}^* D_{X(Y)}/E_{x(y)}^{in}$, we obtain:

$$r_{xx} = \frac{\alpha_x^2}{(\omega - \tilde{\omega}_X)} + \frac{\alpha_x^2 \tilde{\kappa}_{XY}^2}{(\omega - \tilde{\omega}_Y)} + \frac{\alpha_x^2 \tilde{\kappa}_{XQ}^2}{(\omega - \tilde{\omega}_Q')}, \quad (2)$$

$$r_{yy} = \frac{\alpha_y^2}{(\omega - \tilde{\omega}_Y)} + \frac{\alpha_y^2 \tilde{\kappa}_{XY}^2}{(\omega - \tilde{\omega}_X)} + \frac{\alpha_y^2 \tilde{\kappa}_{YQ}^2}{(\omega - \tilde{\omega}_Q')}, \quad (3)$$

where the normalized coupling coefficients $\tilde{\kappa}_{lm}$ between the modes are given by

$$\tilde{\kappa}_{XY} = \frac{\kappa_{XY}}{\tilde{\omega}_X - \tilde{\omega}_Y}, \tilde{\kappa}_{XQ} = \frac{\kappa_{XQ}}{\tilde{\omega}_X - \tilde{\omega}_Q}, \tilde{\kappa}_{YQ} = \tilde{\kappa}_{XY}\tilde{\kappa}_{XQ}. \quad (4)$$

The renormalized/red-shifted frequency ω_Q' and the radiatively reduced lifetime τ_Q' of the DQ mode are approximated as

$$\omega_Q' \approx \omega_Q - \frac{\kappa_{XQ}^2}{(\omega_X - \omega_Q)} - \frac{\kappa_{XY}^2 \kappa_{XQ}^2}{(\omega_X - \omega_Q)^2(\omega_Y - \omega_Q)},$$
$$\frac{1}{\tau_Q'} \approx \frac{1}{\tau_Q^{\rm Ohm}} + \kappa_{XQ}^2 \frac{\alpha_x^2}{(\omega_Q - \omega_X)^2} + \kappa_{XY}^2 \kappa_{XQ}^2 \times$$
$$\frac{\alpha_y^2(\omega_X - \omega_Q)^2 + 2\alpha_x^2(\omega_X - \omega_Q)(\omega_Y - \omega_Q)}{(\omega_X - \omega_Q)^4(\omega_Y - \omega_Q)^2}, \quad (5)$$

where the large modal separation assumption of $|\omega_{X,Y} - \omega_Q| \gg 1/\tau_{X,Y}$ is used.

The two key features of the experimentally measured $R_{xx(yy)} \equiv |r_{xx(yy)}|^2$ reflectivity spectra can now be understood by examining the dependence of the Fano feature's magnitude $r_{xx(yy)}^{\rm Fano}$ on s_y. It is given by the third term in the rhs of Eqs. (2,3) evaluated at $\omega = \omega_Q'$:

$$r_{xx}^{\rm Fano} \propto \frac{\alpha_x^2 s_y^2}{1/\tau_Q^{\rm Ohm} + \beta s_y^2 + \gamma s_y^4}, r_{yy}^{\rm Fano} \propto \frac{\alpha_y^2 s_y^4}{1/\tau_Q^{\rm Ohm} + \beta s_y^2 + \gamma s_y^4}, \quad (6)$$

where β and γ follow from Eq. (5).

We observe that the decay rate of the DCF resonance given by the denominators of Eq.(6) can be broken up into three contributions: (a) the Ohmic (non-radiative) contribution, (b) the contribution $\propto s_y^2$ corresponding to the radiative decay into the x-polarized continuum, and (c) the contribution $\propto s_y^4$ corresponding to the radiative decay into the y-polarized continuum. Depending on the relative dominance of these three mechanisms controlled by s_y, the three respective coupling regimes can be identified as (i) weak coupling regime ($s_y < L_y/4$), (ii) intermediate coupling regime ($L_y/4 < s_y \ll L_y/2$), and (iii) strong coupling regime ($s_y \sim L_y/2$). The transition from weak to strong coupling regimes with increasing s_y explains the decrease of the quality factor of the Fano resonance with s_y evident from Fig. 2(b). The experimentally estimated quality-factors of the DQ mode drop from its Ohmic loss limited value [6] of $Q = 13$ to $Q = 7$ (strong $y-$polarized radiative loss) as s_y increases from $s_y = 0.22\,\mu m$ to $s_y = 1.12\,\mu m$.

The slower emergence of the Fano feature in the R_{yy} spectrum compared with the R_{xx} (*first* observation) can be understood from the scaling of $r_{yy}^{\rm Fano} \propto s_y^4$ versus $r_{xx}^{\rm Fano} \propto s_y^2$ in the weak coupling regime. The situation changes dramatically for $s_y \geq L_y/2$ and the Fano feature in R_{yy} becomes stronger than in R_{xx} because of the $\alpha_y > \alpha_x$ relationship which is the consequence of $L_y > L_x$. The *second* observation is also explained by the non-monotonic dependence of $r_{xx}^{\rm Fano}$ on s_y due to the transition to strong coupling regime, where the continuum state competition [1] in DCF is responsible for the weakening of the Fano feature in R_{xx} for large s_y.

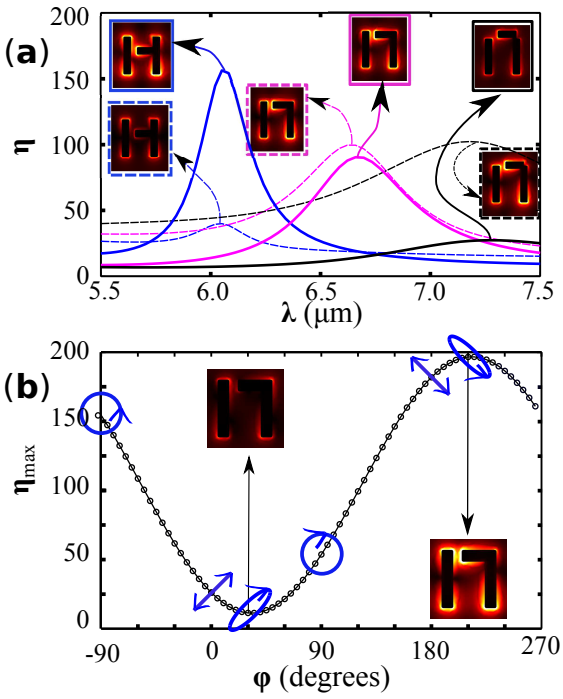

FIG. 3: (color online) COMSOL simulations of the optical intensity enhancement $\eta = \langle|\vec{E}|^2\rangle/E_0^2$ averaged over all (except metal-substrate) metal interfaces in plasmonic DCF metasurfaces. (a) η for $x-$polarized (solid) and $y-$polarized (dashed lines) incident light for weak-coupled ($s_y = 0.32\mu$m), intermediately-coupled ($s_y = 0.72\mu$m), and strongly-coupled ($s_y = 1.14\mu$m) regimes. Insets: near field profiles. (b) The dependence of $\eta_{\rm max}$ on the incident light chirality parametrized by the phase shift ϕ (see text) for the $s_y = 0.52\mu$m metasurface. Insets: near-field intensities for $\phi = 30^\circ$ (left) and $\phi = 210^\circ$ (right). Closed directional loops indicate the polarization state of incident light as a function for $-90^\circ < \phi < 270^\circ$.

Circularly dichroic energy concentration– It has been long recognized that one of the attractions of Fano-resonant metasurfaces is strong optical field enhancement due to the excitation of dark plasmonic resonances. Controlled by the metasurfaces' geometry, those can be utilized for sensing and nonlinear applications. As we demonstrate below, optical field concentration can also be controlled through interference [19] by engineering a general elliptic polarization state of the incident light. The consequences of this effect include giant CD in absorption and transmission [20].

First, we calculate the amplitude Q of the dark resonance in the proximity of the DQ mode in response to the incident light with complex-valued amplitudes $(E_x, E_y) = E_0(1, \exp i\phi)/\sqrt{2}$. Here ϕ is the relative phase between the $x-$ and $y-$ polarizations that determines the state of elliptic polarization as illustrated in Fig. 3(b). At the Fano resonance, the amplitude of the DQ mode is expressed from Eq. (1) as $Q = E_0 \left(q_{xx} + \exp(i\phi) q_{yy}\right) / (\omega - \tilde{\omega}'_Q)$, where

$$q_{xx} = \frac{\alpha_x \ \kappa_{XQ}(s_y)}{\tilde{\omega}_X - \tilde{\omega}_Q}, q_{yy} = \frac{\alpha_y \ \kappa_{XQ}(s_y) \ \kappa_{XY}(s_y)}{(\tilde{\omega}_X - \tilde{\omega}_Q)(\tilde{\omega}_Y - \tilde{\omega}_Q)} \quad (7)$$

are complex-valued field enhancement coefficients.

Because of the different scaling of q_{xx} and q_{yy} with s_y, it follows from Eq. (7) that in the weak (strong) coupling regime the strongest field enhancement is achieved for the $x-$ ($y-$) polarized light. This is confirmed by electromagnetic COMSOL simulations of the surface-averaged optical intensity enhancement $\eta \equiv \langle |\vec{E}|^2 \rangle / E_0^2$ shown in Fig. 3(a) for the $x-$ and $y-$polarized light incident on DCF metasurfaces with different values of s_y. An even more remarkable conclusion derived from Eq. (7) is the possibility of controlling the field enhancement using elliptically-polarized light.

The resulting CD (i.e. the dependence of $\eta \propto |Q|^2$ on ϕ) is the consequence of the finite phase difference $\Delta\phi = \arg(q_{xx}/q_{yy})$: the field enhancement is maximized (minimized) for $\phi_{\max} = \Delta\phi$ ($\phi_{\min} = \Delta\phi + \pi$) due to the constructive (destructive) interference between the two excitation pathways. Moreover, symmetry properties of the coupling coefficients κ_{XQ} and κ_{XY} ensure the following property of the structure's enantiomeric partner produced by displacing of the HCN to the opposite side ($s_y \to -s_y$) of the symmetry plane: $|Q|(\phi, -s_y) = |Q|(\phi + \pi; s_y)$.

These qualitative results are confirmed by COMSOL simulations carried out for the $s_y = 0.52\mu$m structure chosen because $|q_{xx}| \approx |q_{yy}|$ according to Fig. 3(b). The peak enhancement factor $\eta_{\max}(\phi) \equiv \eta(\lambda'_{DQ}, \phi)$ plotted in Fig. 3(b) reveals strong CD. The ratio of the highest ($\phi_{\max} \approx 210°$) to lowest ($\phi_{\min} \approx 30°$) near-field intensities is ≈ 20, and the enhancement ratio for right-hand circularly polarized (RCP) light ($\phi = -90°$) is three times higher than for the left-hand circularly polarized (LCP) light ($\phi = 90°$).

Because $\eta_{\max}(\phi)$ and peak Ohmic loss $A(\phi)$ are proportional to each other, ϕ emerges as a powerful tool for controlling the absorption using the interference of the polarization components of elliptically polarized light. For example, we find for the DCF metasurface shown in Fig. 3(b) that $A(\phi_{\min}) \approx 1.5\%$, i.e. the absorption is coherently suppressed. On the other hand, $A(\phi_{\max}) \approx 41\%$, i.e. the absorption is coherently enhanced almost to the absolute absorption limit ($A_{lim} = 50\%$)of a thin layer in vacuum [21]. Another important consequence of the related giant CD absorbance of the DCF metasurface ($A_{\mathrm{RCP}} = 30\%$ vs $A_{\mathrm{LCP}} = 13\%$) is that it exhibits circular conversion dichroism [20] due to the dissipation asymmetry between RCP and LCP light.

In conclusion, we have demonstrated that a quantum mechanical phenomenon of double continuum Fano (DCF) interference can be classically emulated using an asymmetric plasmonic metasurface. The relative coupling strength between the discrete and two continuum states, distinguished from each other by their polarization, were experimentally varied by changing the degree of symmetry breaking of the metasurface. The phenomenon of continuum state competition, by which one of the continuum states suppresses the Fano resonance for the orthogonal light polarization, was observed and analytically explained. This work opens new possibilities for controlling optical energy concentration on the nanoscale using the chirality of the incident light, thereby providing a simple and powerful tool for developing novel nanophotonic applications such as sensors and detectors.

This work was supported by the Office of Naval Research (ONR) Award N00014-13-1-0837, by the National Science Foundation(NSF) Award DMR 1120923, and by US Army Research Office (ARO) Award W911NF-11-1-0447.

[1] Ugo Fano (1961) Phys. Rev. **1961**, 124, 1866 - 1878
[2] Fan, S.; Joannopoulos, J. D. (2002). Phys. Rev. B **65,** 235112
[3] Fedotov, V. A.; Rose, M.; Prosvirnin, S. L.; Papasimakis, N.; Zheludev, N. I. (2007). Phys. Rev. Lett. **99,** 147401
[4] Miroshnichenko, A. E; Flach, S; Kivshar, Y. S; (2010) Fano resonances in nanoscale structures. Rev. Mod. Phys. **82,** 2257-2298
[5] Luk'yanchuk, B. et al; The Fano resonance in plasmonic nanostructures and metamaterials. Nature Mater. **9,** 707-715 (2010).
[6] N. Liu, L. Langguth, T. Weiss, J. Kastel, M. Fleischhauer, T. Pfau, and H. Giessen '"Plasmonic analogue of electromagnetically induced transparency at the Drude damping limit", Nature Materials **8,** 758 (2009).
[7] Wu et al. Nature Materials "Fano-resonant asymmetric metamaterials for ultrasensitive spectroscopy and identification of molecular monolayers".
[8] F. Hao, Y. Sonnefraud, P. Van Dorpe, S. A. Maier,

N. J. Halas and P. Nordlander; Nano Lett; 2008, 8 (11), pp 39833988 "Symmetry Breaking in Plasmonic Nanocavities: Subradiant LSPR Sensing and a Tunable Fano Resonance"

[9] C.-Y. Chao and L. J. Guo; Appl. Phys. Lett. 83, 1527 (2003); Biochemical sensors based on polymer microrings with sharp asymmetrical resonance

[10] N. Liu, M. L. Tang, M. Hentschel, H. Giessen; '"Nanoantenna-enhanced gas sensing in a single tailored nanofocus", Nature Materials 10, 631636 (2011).

[11] Pendry, J.B.; Holden, A. J.; Robbins, D. J.; and Stewart, W. J. Magnetism from Conductors and Enhanced Nonlinear Phenomena

[12] Benninnk, R. S.; Yoon, Y.-K.; Boyd, R. W.; and Sipe, J. E.; "Accessing the optical nonlinearity of metals with metaldielectric photonic bandgap structures", Opt. Lett. 24, 14161418 (1999).

[13] A. B. Khanikaev, C. Wu, and G. Shvets, "Fano-resonant metamaterials and their applications", Nanophotonics **2,** 247 (2013).

[14] B. Gallinet and O. J. F. Martin,"Ab initio theory of Fano resonances in plasmonic nanostructures and metamaterials", Phys. Rev. B **83,** 235427(2011).

[15] C. Wu, A. B. Khanikaev, and G. Shvets, "Broadband Slow Light Metamaterial Based on a Double-Continuum Fano Resonance", Phys. Rev. Lett. **106,** 107403 (2011).

[16] E. J. Osley, C. G. Biris, P. G. Thompson, R. R. F. Jahromi, P. A. Warburton, and N. C. Panoiu, "Fano Resonance Resulting from a Tunable Interaction between Molecular Vibrational Modes and a Double Continuum of a Plasmonic Metamolecule", Phys. Rev. Lett. **110,** 087402 (2013).

[17] Haus, H; Waves and Fields in Optoelectronics (Prentice-Hall:Englewood Cliffs, NJ, 1984).

[18] S. Fan, W. Suh, and J. D. Joannopoulos, "Temporal Coupled-Mode Theory for Fano Resonance in Light Scattering by a Single Obstacle", J. Opt. Soc. Am. A **20,** 569 (2003).

[19] Y. D. Chong, L. Ge, H. Cao, and A. D. Stone, "Coherent Perfect Absorbers: Time-Reversed Lasers", Phys. Rev. Lett. **105,** 053901 (2010).

[20] V. A. Fedotov, P. L. Mladyonov, S. L. Prosvirnin, A.V. Rogacheva, Y. Chen, and N. I. Zheludev, "Asymmetric Propagation of Electromagnetic Waves through a Planar Chiral Structure", Phys. Rev. Lett. **97,** 167401 (2006).

[21] F. J. Garca de Abajo, "Light scattering by particle and hole arrays", Rev. Mod. Phys. **79,** 1267 (2007).

[22] Chihhui Wu, Nihal Arju, Glen Kelp, Jonathan A. Fan, Jason Dominguez, Edward Gonzales, Emanuel Tutuc, Igal Brener, and Gennady Shvets, "Spectrally selective chiral silicon metasurfaces based on infrared Fano resonances", Nature Communications (2014).

[23] S. Hossein Mousavi, Iskandar Kholmanov, Kamil B. Alici, David Purtseladze, Nihal Arju,Kaya Tatar, David Y. Fozdar, Ji Won Suk, Yufeng Hao, Alexander B. Khanikaev, Rodney S. Ruoff, and Gennady Shvets, "Inductive Tuning of Fano-Resonant Metasurfaces Using Plasmonic Response of Graphene in the Mid-Infrared", Nano Letters **13,** 1111 (2013).

[24] Alonso-Gonzalez, Pablo and Schnell, Martin and Sarriugarte, Paulo and Sobhani, Heidar and Wu, Chihhui and Arju, Nihal and Khanikaev, Alexander and Golmar, Federico and Albella, Pablo and Arzubiaga, Libe and Casanova, Felix and Hueso, Luis E. and Nordlander, Peter and Shvets, Gennady and Hillenbrand, Rainer "Real-Space Mapping of Fano Interference in Plasmonic Metamolecules," Nano Letters, 11(9), pp. 3922-3926 (2011)

[25] Maier, S. A.; Atwater, H. A. J. Appl. Phys. 2005, 98, 011101.

[26] Mock, J. J.; Barbic, M.; Smith, D. R.; Schultz, D. A.; Schultz, S. J. Chem. Phys. 2002, 116, 67556759.

[27] Kuwata, H.; Tamaru, H.; Esumi, K.; Miyano, K. Appl. Phys. Lett. 2003, 83, 46252627.

[28] Niels Verellen,Yannick Sonnefraud, Heidar Sobhani, Feng Hao, Victor V. Moshchalkov, Pol Van Dorpe,Peter Nordlander, and Stefan A. Maier; Nano Lett. 9(4) 1663-1667

[29] Kneipp, K.; Kneipp, H.; Itzkan, I.; Dasari, R. R.; Feld, M. S. J. Phys.: Condens. Matter 2002, 14, R597-R624.

[30] Xu, H.; Aizpurua, J.; Kaell, M.; Apell, P. Phys. ReV. E 2000, 62, 4318 4324.

[31] Anker, J. N.; Hall, W. P.; Lyandres, O.; Shah, N. C.; Zhao, J.; Duyne, R. P. V. Nat. Mater. 2008, 7, 442453.

[32] Lal, S.; Clare, S. E.; Halas, N. J. Acc. Chem. Res. 2008, 41, 1842 1851.

[33] Na Liu, Mario Hentschel, Thomas Weiss, A. Paul Alivisatos1, Harald Giessen; Science; Vol. 332 no. 6036 pp. 1407-1410;

[34] Christopher Tabor, Raghunath Murali, Mahmoud Mahmoud and Mostafa A. El-Sayed; J. Phys. Chem. A, 2009, 113 (10), pp 19461953

[35] Bergman, D. J.; Stockman, M. I. Phys. ReV. Lett. 2003, 90, 027402.

[36] Zheludev, N. I.; Prosvirnin, S. L.; Papasimakis, N.; Fedotov, V. A. Nat. Photon. 2008, 2, 358.

[37] P. Weis, O. Paul, C. Imhof, R. Beigang, and M. Rahm "Strongly birefringent metamaterials as negative index terahertz wave plates" Applied Physics Letters 95, 171104 (2009)

[38] A. E. etin, Ahmet Ali Yanik, Cihan Yilmaz, Sivasubramanian Somu, Ahmed Busnaina, and Hatice Altug; "Monopole antenna arrays for optical trapping, spectroscopy, and sensing" Appl. Phys. Lett. 98, 111110 (2011)

[39] R. Adato, A. Yanik, and Hatice Altug "On Chip Plasmonic Monopole Nano-Antennas and Circuits" Nano Letters 11, pp 5219 (2011)

[40] Richard Taubert, Mario Hentschel, Jrgen Kstel, and Harald Giessen "Classical Analog of Electromagnetically Induced Absorption in Plasmonics" Nano Letters 12, pp 1367

[41] S. Hossein Mousavi, Alexander B. Khanikaev, Burton Neuner III, David Y. Fozdar, Timothy D. Corrigan, Paul W. Kolb, H. Dennis Drew, Raymond J. Phaneuf, Andrea Alu, and Gennady Shvets "Suppression of long-range collective effects in meta-surfaces formed by plasmonic antenna pairs" Optics Express 19, pp 22142

[42] Ruan, Z; Fan, S. "Temporal Coupled-Mode Theory for Fano Resonance in Light Scattering by a Single Obstacle" J. Phys. Chem. C 114, 73247329 (2010)

[43] Liu, N; Mesch, M; Weiss, T; Hentschel, M; Giessen, H. (2010). Infrared perfect absorber and its application as plasmonic sensor. Nano letters, 10(7), 2342-2348.